

# PCE-Based Approach to Worst-Case Scenario Analysis in Wireless Telecommunication Systems

Piotr Górniki\* and Wojciech Bandurski

**Abstract**—In the paper, we present a novel PCE-based approach for the effective analysis of worst-case scenario in a wireless telecommunication system. Usually, in such analysis derivation of polynomial chaos expansion (PCE meta-model) of a considered EM field function for one precise set of probability densities of random variables does not provide enough information. Consequently, a number of PCE meta-models of the EM field function should be derived, each for the different joint probability density of a vector of random variables, e.g., associated with different mean (nominal) values of random variables. The general polynomial chaos (gPC) approach requires numerical calculations for each PCE meta-model derivation. In order to significantly decrease the time required to derive all of the PCE meta-models, the novel approach has been introduced. It utilizes the novel so-called primary approximation and the novel analytical formulas. They significantly decrease the number of numerical calculations required to derive all of the PCE meta-models compared with the gPC approach. In the paper, we analyze the stochastic EM fields distributions in a telecommunication system in a spatial domain. For this purpose, analysis of uncertainties associated with a propagation channel as well as with transmitting and receiving antennas was introduced. We take advantage of a ray theory in our analysis. This allows us to provide the novel method for rapid calculation of a PCE meta-model of a telecommunication system transfer function by using the separate PCE meta-models associated with antennas and a propagation channel.

## 1. INTRODUCTION

Simulations of electromagnetic (EM) fields cover many subjects in the area of antenna analysis and EM wave propagation prediction, e.g., [1–8]. It is often important to include the random behavior of parameters of a considered scenario in these simulations. This way, we can model, e.g., uncertainties of physical parameters of a simulated system.

One of the best-known methods of including random behavior of parameters of a given scenario in EM field simulations is the Monte Carlo method, e.g., [9, 10]. In this method, simulations are performed consecutively for variables values drawn according to an assumed probability distribution, e.g., Gaussian, Beta or uniform distributions. This method provides high accuracy in determining probability distributions of EM fields; however, it requires a lot of iterations to obtain satisfyingly accurate results. An alternative method to the Monte Carlo algorithm is the application of polynomial chaos expansion (PCE) which originates from the work of Norbert Wiener in 1938 [11] and since then was discussed in numerous articles and books, and widely used in scientific engineering, including electromagnetics, e.g., [12–17]. Our work, according to the best knowledge of the authors, is the first in which the total impact of uncertainties associated with antennas and the propagation channel on the distribution of a random electromagnetic field in a telecommunication system is analyzed. PCE enables a sufficient decrease in the computation time required to calculate the stochastic results of functions of random variables. The use of PCE for the analysis and simulation of stochastic linear systems in the

---

*Received 20 March 2019, Accepted 8 July 2019, Scheduled 17 July 2019*

\* Corresponding author: Piotr Górniki (piotr.gorniki@put.poznan.pl).

The authors are with the Department of Electronics and Telecommunications, Poznan University of Technology, Poland.

frequency-domain is based on two methods: Galerkin projection and collocation. These methods can also be used for nonlinear systems in the time-domain; however, such a case will not be considered in this work.

PCE method utilizing Galerkin projection is based on the calculation of expansion coefficients that are used to calculate statistics of considered distributions [13, 14]. The Galerkin projection has a number of convenient analytic features that make them attractive for use within analyses that extend beyond the traditional process of determining the effect of uncertainties of system physical parameters on the system response, such as local and global sensitivity analysis and design under uncertainty algorithms [18].

The collocation method requires only repetitive executions of existing deterministic solvers, so it is non-intrusive and may thus be faster [19]. However, an important issue to be kept in mind is that the aliasing errors in stochastic collocation can be significant, especially, again, for higher dimensional random spaces [19]. This indicates that the Galerkin method offers the most accurate solution of PCE coefficients of the considered function of random variables. For further comparisons of these two methods see, e.g., [12, 18, 19].

In our work, we focus on the worst-case analysis of EM field in a wireless telecommunication system for an environment whose geometrical and/or material parameters can change, for various reasons, in a random manner. This analysis is preferably carried out, as we justified above, based on the PCE method using the Galerkin projection. In this approach, the most time-consuming operation is to calculate the appropriate number of expansion coefficients in a series of orthogonal polynomials. As it is known, the number of coefficients affects the accuracy of the method, because on their basis, statistics of the stochastic process such as the average or standard deviation, etc. are calculated.

The worst-case analysis of stochastic EM field in a wireless telecommunication system requires to perform stochastic analysis repeatedly because during such analysis it is necessary to change probability density functions and/or the ranges of variation, as well as nominal values of random parameters of transmitting and receiving antennas and a propagation channel. When we have to calculate the mentioned coefficients in the PCE method repeatedly, the calculation time dramatically increases.

Our aim is to avoid this serious inconvenience by introducing the universal PCE-based approach utilizing primary approximation and the new closed-form polynomial chaos coefficients, which we call Universal Expansion Coefficients (UECs). We use the word “universal” to call our approach and our explicit analytical formulas, because in our opinion any of the nowadays intrusive or non-intrusive methods for PCE coefficients calculation can be implemented to the primary approximation which is one of the key elements of our new approach. The main idea of the proposed approach is to notice that stochastic polynomials associated with the most common probability density functions in such pairs as normal distribution — Hermite polynomials, Beta distribution — Jacobi polynomials [12, 19], etc. can be expanded in series relative to each other, and the coefficients of these expansions can be calculated by means of analytical integration resulting in known analytical relationships [20–22]. Thanks to the use of this property, we can calculate the coefficients in the PCE method only once, regardless of changes in the types of probability density function and/or variation of ranges of random parameters, what significantly shortens the simulation times in the case described above.

Let us stress that UECs have to be calculated of course but only once during the process of so-called primary approximation of the functions associated with a simulated wireless telecommunication system. In our approach, changing the values of random variables (e.g., an average and a standard deviation) or changing the range of a random variable (e.g., a random variable range for a Beta distribution) does not require, as it was already noted above, recalculation of the expansion coefficients through direct numerical integration or linear regression, which must be done for each frequency. The introduced UECs can be recalculated, as it was mentioned, using explicit analytical formulas [20–22].

In order to introduce our new approach for wireless telecommunication system analysis, it is convenient and natural to adopt the system theory language for modeling the mentioned wireless telecommunication system in which we distinguish transfer functions of antennas and a propagation channel. A similar approach has been applied for stochastic microwave systems with the use of n-port description, e.g., [23]. Transfer functions can be obtained from an analytical description in the frequency-domain, e.g., ray theory including UTD or by means of an approximation method (e.g., vector fitting) using frequency-domain samples obtained from a measurement or from a full-wave EM field simulator.

The adoption of system theory approach allows the decrease of required PCE expansions order what greatly accelerates the simulation of a wireless telecommunication system.

The new results enable us to effectively analyze simulation scenarios where many (up to 10 in our simulation examples) independent random variables can be considered.

The paper is organized as follows. In Section 2, we recall the mathematical background of the PCE method and formulate the problem that is addressed in the paper. In Section 3, we present the algorithm of our UECs approach. We present the concept of the so-called primary approximation and derive polynomial chaos UECs for multiple random variables having Gaussian and Beta probability densities. We demonstrate the usefulness of system approach adoption to the considered telecommunication system. In Section 4, we use UTD ray theory and our UECs approach to mentioned worst-case analysis in a wireless telecommunication system for an exemplary scenario of diffraction of an EM wave on convex obstacles. We conclude the paper in Section 5.

## 2. STATEMENT OF THE PROBLEM

We recall the basic theory about PCE related to stochastic analysis. Using the general Polynomial Chaos theory (gPC) [12] we can expand the function of random variables associated with a simulated system using PCE coefficients with a polynomial basis which is orthogonal with respect to probability density (PDF) of the random variables [12]. If we assume that the transfer function  $HT(\omega, \boldsymbol{\xi})$  associated with the simulated telecommunication system depends on  $d$  independent random variables given by vector  $\boldsymbol{\xi} = \{\xi_0, \xi_1, \dots, \xi_{d-1}\}$ , then the expansion of  $HT(\omega, \boldsymbol{\xi})$  for pulsation sample no.  $s$  can be written as:

$$HT(\omega_s, \boldsymbol{\xi}) \approx \sum_{\mathbf{k}} A_{\mathbf{k},s} \prod_{n=0}^{d-1} \varphi_{k_n}(\xi_n) \quad (1)$$

where  $\mathbf{k} = \{k_0, k_1, \dots, k_{d-1}\}$  is a multi-index. The order of multi-indexes can be found using the Askey scheme [12], while expansion coefficients  $A_{\mathbf{k},w}$ , using the Galerkin projection [12], are:

$$A_{\mathbf{k},w} = \left\langle HT(\omega_s, \boldsymbol{\xi}), \prod_{n=0}^{d-1} \varphi(\xi_n) \right\rangle = \frac{\int_{a_0}^{b_0} \dots \int_{a_{d-1}}^{b_{d-1}} HT(\omega_s, \boldsymbol{\xi}) \prod_{n=0}^{d-1} \varphi(\xi_n) \prod_{n=0}^{d-1} p_n(\xi_n) d\xi_{d-1} \dots d\xi_0}{\gamma_{\mathbf{k}}} \quad (2)$$

where  $\varphi(\xi_n)$  is the  $k_n$ -th element of the basis of polynomials that are orthogonal for probability density functions  $p_n(\xi_n)$  of random variables  $\xi_n$  in domain limits  $a_n \leq \xi_n \leq b_n$ , and  $\gamma_{\mathbf{k}} = \gamma_0 \cdot \gamma_1 \cdot \dots \cdot \gamma_{d-1}$  is a multi-normalization factor [12], while  $k_n$  is the  $n$ -th element of multi-index  $\mathbf{k}$ . It should be noticed that for Gaussian distribution numerical integration of Eq. (2) can be in practice truncated and consequently performed within finite limits, e.g.,  $(\mu - 5\sigma, \mu + 5\sigma)$ , here  $\mu$  and  $\sigma$  are the mean and standard deviation of a Gaussian PDF. Using the expansion coefficients in Eq. (2) the mean and standard deviation of random transfer function  $HT(\omega, \boldsymbol{\xi})$  for pulsation samples  $\omega_s$  can be found as follows [12]:

$$\mu_w = A_{\{0,0,\dots,0\},w} \quad (3)$$

$$\sigma_w = \sqrt{\sum_{\mathbf{k} \neq \{0,0,\dots,0\}} \gamma_{\mathbf{k}}^2 \cdot A_{\mathbf{k},w}^2} \quad (4)$$

We address in the paper the problem of worst-case analysis in the wireless telecommunication system. The transfer function of a telecommunication system with random parameters can be written as follows:

$$HT(\omega, \boldsymbol{\xi}) = \sum_{r=1}^R HC_r^{\text{ATFs}}(\omega, \boldsymbol{\xi}_r^{\text{ATFs}}) \cdot HC_r^{\text{CTF}}(\omega, \boldsymbol{\xi}_r^{\text{CTF}}) \quad (5)$$

where  $HC_r^{\text{ATFs}}(\omega, \boldsymbol{\xi}_r^{\text{ATFs}})$  is the joint transfer function of transmitting and receiving antennas associated with the  $r$ -th ray path which originates at the point of EM field source and ends at the observation point;  $HC_r^{\text{CTF}}(\omega, \boldsymbol{\xi}_r^{\text{CTF}})$  is the corresponding transfer function of the  $r$ -th ray;  $\boldsymbol{\xi}_r^{\text{ATF}}$  is the vector of

random variables of antennas transfer functions corresponding to  $r$ -th ray path, while  $\xi_r^{\text{CTF}}$  is the vector of random variables of transfer function of the  $r$ -th ray. It is possible that transfer functions  $HC_r^{\text{CTF}}(\omega, \xi_r^{\text{CTF}})$  depend on the same vector of random variables, e.g., when rays interact with the same obstacles or it is assumed that parameters of obstacles are deterministic, while antenna positions are random variables.

In order to define the problem of worst-case analysis in a telecommunication system, we define support  $\Omega^0$  of random variables  $\xi$  for which the worst-case analysis need to be made. This support can be associated, e.g., with limits of spatial coordinates of antennas positions. Then support  $\Omega^0$  is sampled into much smaller supports, e.g., supports  $\Omega_v$ ,  $v \in \{1, 2, \dots, V\}$  which correspond to a selected set of nominal values of  $\xi$ . Supports  $\Omega_v$  need to reflect uncertainties which can be met in a real life, e.g., uncertainty in determining the position of antennas. We assume that each of supports  $\Omega_v$  can be associated with Gaussian, Beta or Uniform PDF. After support  $\Omega^0$ , supports  $\Omega_v$  and associated PDFs are chosen, we perform simulations of considered telecommunication system repeatedly. In the gPC approach, we need to perform a numerical calculation of PCE coefficients for every execution of the simulation. The diagram showing this approach can be presented as follows.

### 3. THE UEC APPROACH

#### 3.1. The Diagram of the UEC Approach

When the worst-case analysis in a telecommunication system is performed according to the algorithm shown in Fig. 1, the calculation time can be not acceptable, because it grows fast, as the simulations of stochastic EM field propagation are repeated. It is the consequence of repeated numerical calculations of PCE coefficients for every support  $\Omega_v$ . We present now the diagram of our UEC approach which ensures substantial reduction of computation times of worst-case analysis in a telecommunication system. The novel blocks in the diagram are indicated by red frames. The diagram can be presented as in Fig. 2.

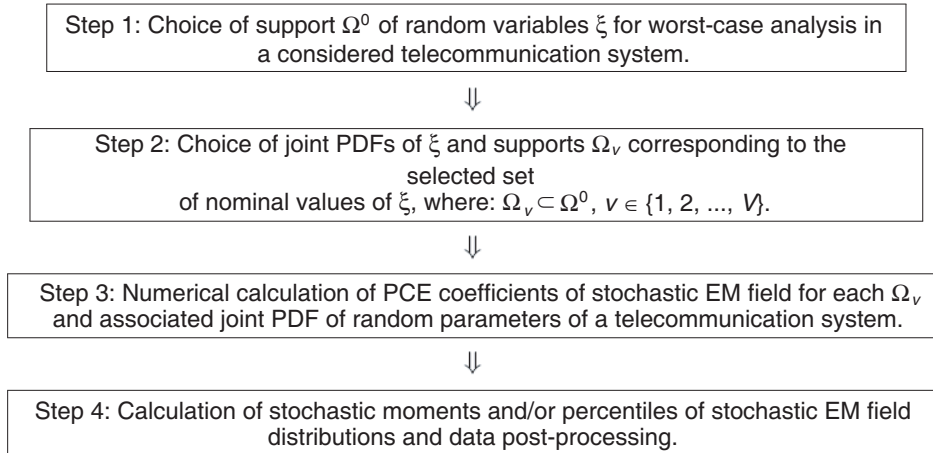


**Figure 1.** The diagram of the gPC approach for worst-case analysis in a telecommunication system.

The first two steps of the UEC approach are the same as in the gPC approach. In the first step of the novel part of the UEC approach, we assign an appropriate subset of variables  $\xi$  to antennas transfer function as it is indicated in (5). The complementary subset of variables is assigned to transfer functions of rays. It should be noted that vectors  $\xi_r^{\text{ATFs}}$  and  $\xi_r^{\text{CTF}}$  do not overlap. We also decompose support of variables  $\xi$  into supports  $\Omega_r^{0,\text{ATFs}}$  and  $\Omega_r^{0,\text{CTF}}$  for variables  $\xi_r^{\text{ATFs}}$  and  $\xi_r^{\text{CTF}}$ , respectively.

In the next step, we divide support  $\Omega_r^{0,\text{CTF}}$  into  $U_r$  supports  $\Omega_{r,u_r}^{0,\text{CTF}}$  for the transfer function of each ray. The number of these supports is the same for each ray when the transfer function of each ray depends on the same vector of random variables. The purpose of this division is to enable relatively fast calculations of accurate primary approximations of ray transfer functions for smaller supports. In

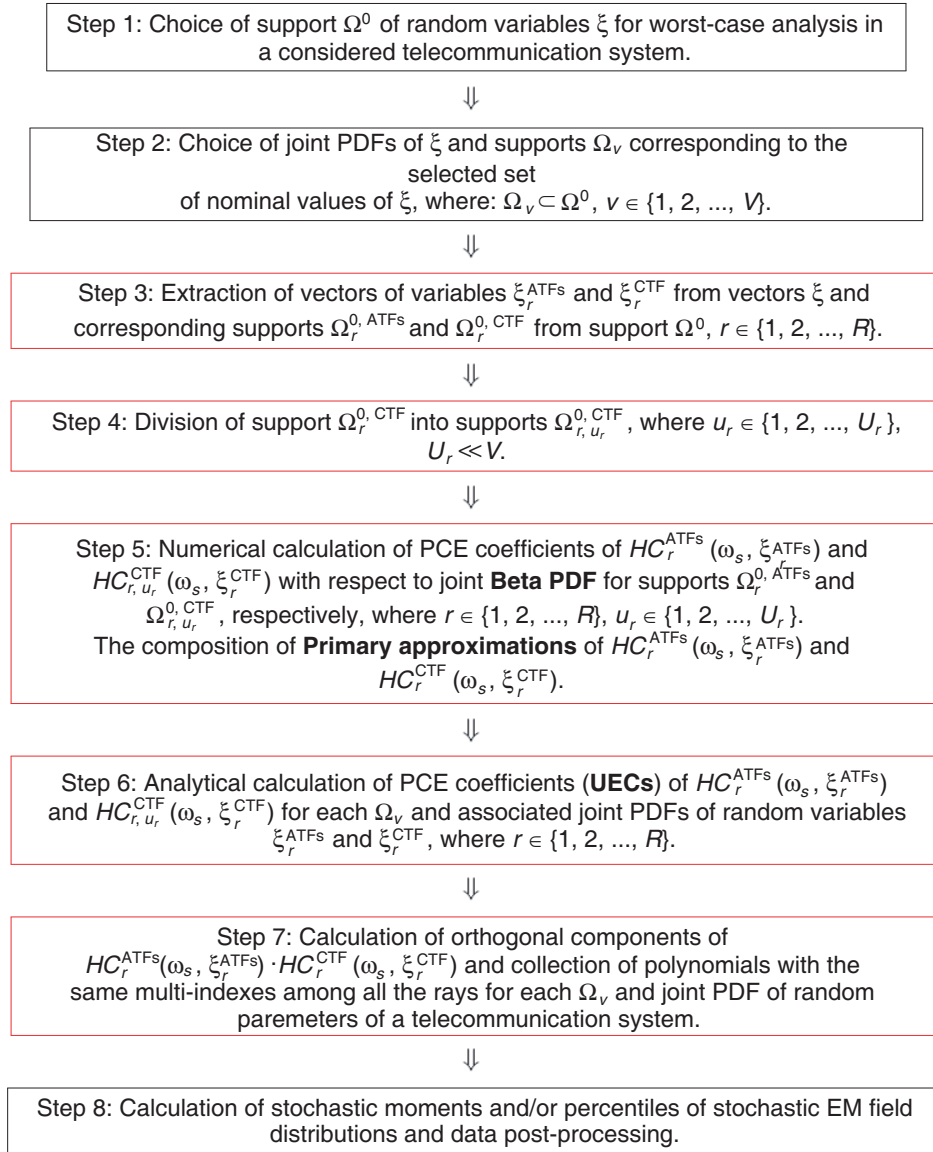


**Figure 2.** The diagram of the UEC approach for worst-case analysis in a wireless telecommunication system.

particular, we need to divide the portion of support  $\Omega_{r,u_r}^{0,CTF}$  which corresponds to spatial coordinates. The results of numerical experiments, which was performed by us for 2 spatial dimensions, indicate that a good choice for the spatial area included in  $\Omega_{r,u_r}^{0,CTF}$  is  $4 - 16\lambda^2$ , where  $\lambda$  is a wavelength. It is not required to divide the support  $\Omega_r^{0,ATFs}$  because it does not include spatial coordinates, therefore dynamics of variation of  $HC_r^{ATFs}(\omega_s, \xi_r^{ATFs})$  is much lower than for the case of transfer function  $HC_r^{CTF}(\omega_s, \xi_r^{CTF})$ . We used the Matlab-based package called UQLab [24] to perform the mentioned numerical experiments.

When primary approximations of  $HC_r^{ATFs}(\omega_s, \xi_r^{ATFs})$  and  $HC_r^{CTF}(\omega_s, \xi_r^{CTF})$  are derived we can apply them to explicit analytical formulas, called UECs, which are the PCE coefficients of  $HC_r^{ATFs}(\omega_s, \xi_r^{ATFs})$  and  $HC_r^{CTF}(\omega_s, \xi_r^{CTF})$  for supports  $\Omega_v$  and selected joint PDFs of  $\xi_r^{ATFs}$  and  $\xi_r^{CTF}$ .

The final step of the novel part of the UEC approach is the derivation of PCE of each transfer function associated with the path of ray no.  $r$ , as well as the collection of polynomials with the same multi-indexes in order to obtain the PCE of a telecommunication system transfer function.

We present the mathematical background of the previewed steps in the next subsections.

### 3.2. The Primary Approximation

In order to derive the universal expansion coefficients (UECs), we present the primary approximation which was introduced in the previous subsection.

The primary approximation of an exemplary transfer function  $HC(\omega, \boldsymbol{\xi})$  for pulsation sample  $\omega_s$  by analogy to Eq. (1) is as follows:

$$HC(\omega_s, \boldsymbol{\xi}) \approx \sum_{\mathbf{q}} C_{\mathbf{q},w} \prod_{n=0}^{d-1} P_{q_n}^{\alpha_0, \beta_0}(f_1(\xi_n)) \quad (6)$$

where  $q_n$  is the  $n$ -th element of multi-index  $\mathbf{q}$ ,

$$f_1(\xi_n) = \xi_n \frac{2}{b_n - a_n} - \frac{b_n + a_n}{b_n - a_n}, \quad f_1(a_n) = -1, \quad f_1(b_n) = 1 \quad (7)$$

and  $P_{q_n}^{\alpha_0, \beta_0}(\xi_n)$  is a Jacobi polynomial of the  $q_n - th$  order with shape parameters  $\alpha_0$  and  $\beta_0$ , while  $a_n$  and  $b_n$  are the lower and higher limits of primary approximation for variable  $\xi_n$ . It should be noted that the number of coefficients  $C_{\mathbf{q},w}$  in Eq. (6) is a finite and minimal number that satisfies the accepted approximation error criterion. We chose this polynomial basis, as we obtained the best approximation results in our experiments using Jacobi polynomials, especially for transfer functions whose specified domains are limited. Coefficients  $C_{\mathbf{q},w}$  can be calculated using Galerkin projection as follows:

$$\begin{aligned} C_{\mathbf{q},w} &= \frac{1}{\gamma_{\mathbf{k}}} \left\langle HC(\omega_s, \{f_2(\xi_0), \dots, f_2(\xi_{d-1})\}), \prod_{n=0}^{d-1} P_{q_n}^{\alpha_0, \beta_0}(\xi_n) \right\rangle \\ &= \frac{1}{\gamma_{\mathbf{k}}} \int_{-1}^1 \dots \int_{-1}^1 HC(\omega_s, \{f_2(\xi_0), \dots, f_2(\xi_{d-1})\}) \prod_{n=0}^{d-1} P_{q_n}^{\alpha_0, \beta_0}(\xi_n) \prod_{n=0}^{d-1} p_n^{Beta}(\alpha_0, \beta_0, \xi_n) d\xi_{d-1} \dots d\xi_0 \quad (8) \end{aligned}$$

where

$$f_2(\xi_n) = \xi_n \frac{b_n - a_n}{2} + \frac{b_n + a_n}{2}, \quad f_2(-1) = a_n, \quad f_2(1) = b_n \quad (9)$$

$$p_n^{Beta}(\alpha, \beta, \xi) = 2^{(\alpha+\beta+1)} \frac{\Gamma(\alpha + \beta + 2)}{\Gamma(\alpha + 1)\Gamma(\beta + 1)} (1 - \xi)^\alpha (1 + \xi)^\beta \quad (10)$$

However, other methods for calculation of PCE coefficients can be used. We use UQLab [24] for numerical calculation of  $C_{\mathbf{q},w}$ . Among several options of PCE coefficients calculation in UQLab, we chose orthogonal matching pursuit (OMP) which is connected with Sobol indices calculation.

The necessary but time-consuming numerical calculations required to obtain coefficients  $C_{\mathbf{q},w}$  are performed for freely chosen parameters  $\alpha_0$  and  $\beta_0$  and only once for a given  $HC(\omega_s, \boldsymbol{\xi})$ . We use  $\alpha_0 = \beta_0 \leq 1$  for the best primary approximation results.

### 3.3. The Universal Expansion Coefficients

Coefficients  $C_{\mathbf{q},w}$  from the previous subsection are tabulated and used to derive our universal expansion coefficients (UECs). We limit our consideration to the case of random variable  $\xi_n$  that can have Gaussian or Beta distribution. Beta distribution enables modeling a symmetric and asymmetric PDF, as well as the uniform PDF. Let new arbitrary parameters of Gaussian probability density function of  $\xi_n$  are mean  $\mu_n$  and standard deviation  $\sigma_n$ . The appropriate parameters of Beta distribution are shape parameters  $\alpha_n$  and  $\beta_n$  while their new ranges are  $c_n \leq \xi_n \leq d_n$  [12]. Then UECs, denoted by  $U_{\mathbf{k},w}$ , are the polynomial chaos expansion coefficients of  $HC(\omega_s, \boldsymbol{\xi})$  with respect to chosen probability distributions of random variables  $\boldsymbol{\xi}$ . The expansion formula with UECs takes the form:

$$HC(\omega_s, \boldsymbol{\xi}) \approx \sum_{\mathbf{k}} U_{\mathbf{k},w} \prod_{n=0}^{d-1} \varphi_{k_n}(f_3(\xi_n)) \quad (11)$$

where  $\varphi_{k_n}(\xi_n)$  can be a Hermite or Jacobi polynomial for Gaussian or Beta distribution, respectively [12]. Function  $f_2(\xi_n)$  for Gaussian distribution is:

$$f_3^G(\xi_n) = \frac{\xi_n - \mu_n}{\sigma_n} \tag{12}$$

while for Beta distribution, by analogy to Eq. (7), we have:

$$f_3^B(\xi_n) = \xi_n \frac{2}{d_n - c_n} - \frac{d_n + c_n}{d_n - c_n} \quad f_3(c_n) = -1 \quad f_3(d_n) = 1 \tag{13}$$

It should be noted that the number of multi-indexes  $\mathbf{k}$  is not higher than the number of multi-indexes  $\mathbf{q}$  because the range of possible values of  $\xi_n$  in Eq. (11) must be a subset of the range of  $\xi_n$  for which the primary approximation in Eq. (6) was derived. The range of possible values of  $\xi_n$  for the case of Beta distribution is  $c_n \leq \xi_n \leq d_n$  but also for the case of a Gaussian distribution this range can in practice be limited to  $\mu_n - M \cdot \sigma_n \leq \xi_n \leq \mu_n + M \cdot \sigma_n$ . We use  $M = 5$  (the UECs are valid for such an assumption). When we take advantage of the primary approximation in Eq. (6) and use the Galerkin projection, the initial formula for our UECs takes the form:

$$U_{\mathbf{k},w} \approx \frac{1}{\gamma_{\mathbf{k}}} \left\langle \sum_{\mathbf{q}} C_{\mathbf{q},w} \prod_{n=0}^{d-1} P_{q_n}^{\alpha_0, \beta_0}(f_1(f_4(\xi_n))), \prod_{n=0}^{d-1} \varphi_{k_n}(\xi_n) \right\rangle \tag{14}$$

Function  $f_4(\xi_n)$  for Gaussian distribution is:

$$f_4^G(\xi_n) = \sigma_n \cdot \xi_n + \mu_n \tag{15}$$

while for Beta distribution, by analogy to Eq. (9), we have:

$$f_4^B(\xi_n) = \xi_n \frac{d_n - c_n}{2} + \frac{d_n + c_n}{2}, \quad f_4(-1) = c_n, \quad f_4(1) = d_n \tag{16}$$

Then we transform a Jacobi polynomial of the  $q_n$ -th order in Eq. (14) into a sum of Hermite polynomials of maximum order  $q_n$ -th [25]. After the transformation, Eq. (14) takes the following form:

$$U_{\mathbf{k},w} \approx \frac{1}{\gamma_{\mathbf{k}}} \left\langle \sum_{\mathbf{q}} D_{\mathbf{q},w} \prod_{n=0}^{d-1} H_{q_n}(f_1(f_4(\xi_n))), \prod_{n=0}^{d-1} \varphi_{k_n}(\xi_n) \right\rangle \tag{17}$$

where  $H_l(x)$  is a Hermite polynomial of order  $l$  and:

$$D_{\mathbf{q},w} = D_{\{q_0, q_1, \dots, q_{d-1}\}, w} = \sum_{i_0 \geq q_0, i_1 \geq q_1, \dots, i_{d-1} \geq q_{d-1}} C_{\{i_0, i_1, \dots, i_{d-1}\}, w} \prod_{n=0}^{d-1} B_{q_n}^{i_n} \tag{18}$$

where  $B_{q_n}^{i_n}$  is the weight of Jacobi polynomial of order  $i_n$ -th that compose a Hermite polynomial of order  $q_n$ -th and can be calculated as in [21].

The UEC in Eq. (17) can be given in the following form:

$$U_{\mathbf{k},w} \approx \frac{1}{\gamma_{\mathbf{k}}} \sum_{\mathbf{q}} D_{\mathbf{q},w} \prod_{n=0}^{d-1} S_{k_n, q_n}(\xi_n) \tag{19}$$

When  $\xi_n$  has Gaussian distribution, then factor  $S_{k_n, q_n}(\xi_n)$  takes the form:

$$S_{k_n, q_n}^G(\xi_n) = \int_{-\infty}^{+\infty} H_{q_n}(f_1(f_4^G(\xi_n))) H_{k_n}(\xi_n) \frac{e^{-\frac{\xi_n^2}{2}}}{\sqrt{2\pi}} d\xi_n \tag{20}$$

while for Beta distribution we have:

$$S_{k_n, q_n}^B(\xi_n) = \int_{-1}^1 H_{q_n}(f_1(f_4^B(\xi_n))) P_{k_n}^{\alpha_n, \beta_n}(\xi_n) p_n^{Beta}(\alpha_n, \beta_n, \xi_n) d\xi_n \tag{21}$$

After simplifying Eqs. (20) and (21), factor  $S_{k_n, q_n}(\xi_n)$  for Gaussian distribution takes the following form:

$$S_{k_n, q_n}^G(\xi_n) = \int_{-\infty}^{+\infty} H_{q_n}(z_D^{\text{Gauss}}(\xi_n)) H_{k_n}(\xi_n) \frac{e^{-\frac{\xi_n^2}{2}}}{\sqrt{2\pi}} d\xi_n \quad (22)$$

where

$$z_D^{\text{Gauss}}(\xi_n) = g_n^{\text{Gauss}} \cdot \xi_n + h_n^{\text{Gauss}} \quad (23)$$

$$g_n^{\text{Gauss}} = \frac{2\sigma_n}{b_n - a_n} \quad (24)$$

$$h_n^{\text{Gauss}} = \frac{2\mu_n - b_n - a_n}{b_n - a_n} \quad (25)$$

while for Beta distribution we have:

$$S_{k_n, q_n}^B(\xi_n) = \int_{-1}^1 H_{q_n}(z_D^{\text{Beta}}(\xi_n)) P_{k_n}^{\alpha_n, \beta_n}(\xi_n) p_n^{\text{Beta}}(\alpha_n, \beta_n, \xi_n) d\xi_n \quad (26)$$

where

$$z_D^{\text{Beta}}(\xi_n) = g_n^{\text{Beta}} \cdot \xi_n + h_n^{\text{Beta}} \quad (27)$$

$$g_n^{\text{Beta}} = \frac{d_n - c_n}{b_n - a_n} \quad (28)$$

$$h_n^{\text{Beta}} = \frac{d_n + c_n - b_n - a_n}{b_n - a_n} \quad (29)$$

The Hermite polynomial of the sum of arguments has the following property [26]:

$$H_l(x + y) = \sum_{j=0}^l \binom{l}{j} x^{l-j} H_j(y) \quad (30)$$

We apply the above property to Eq. (22) with substitutions  $x = h_n^{\text{Gauss}}$ ,  $y = g_n^{\text{Gauss}} \cdot \xi_n$ , as well as to Eq. (26) with substitutions  $x = g_n^{\text{Beta}} \cdot \xi_n$ ,  $y = h_n^{\text{Beta}}$ . When we apply the results of integrals of the forms  $\int_{-\infty}^{\infty} H_{l_1}(z) H_{l_2}(z) \exp(-0.5z^2) dz$  and  $\int_{-1}^1 z^p H_{l_1}(z) P_{l_2}^{\alpha, \beta}(1-z)^\alpha (1+z)^\beta dz$ , as well as subsequent transformations, we derive the closed form formulas for  $S_{k_n, q_n}(\xi_n)$ . For  $\xi_n$  with Gaussian PDF, we have:

$$S_{k_n, q_n}^G(\xi_n) = \left( \frac{h_n^{\text{Gauss}}}{\sqrt{1 - (g_n^{\text{Gauss}})^{-2}}} \right)^{k_n} \cdot \sum_{j=0}^{k_n} \left( \sqrt{\frac{(g_n^{\text{Gauss}})^2 - 1}{(h_n^{\text{Gauss}})^2}} \right)^j Q(j, q_n, k_n) \quad (31)$$

where  $Q(j, q_n, k_n)$  does not depend on  $\mu_n$  or  $\sigma_n$ , therefore, they can be tabulated as follows. When  $(j - k_n) = 0, 2, 4, 6, \dots$ , we have [21]:

$$Q(j, q_n, k_n) = \frac{q_n!}{(q_n - j)! \left( \frac{j - k_n}{2} \right)! (\sqrt{2})^{j - k_n}} \quad (32)$$

while Eq. (32) is 0 for the remaining values of  $(j - k_n)$ . The corresponding formula to Eq. (31) for the case of Beta PDF is:

$$S_{k_n, q_n}^B(\xi_n) = \sum_{j=0}^{q_n} \binom{q_n}{j} H_j(h_n^{\text{Beta}}) (g_n^{\text{Beta}})^{q_n - j} I_n \quad (33)$$

where  $I_n$  is 0 for  $q_n - j < k_n$ , and for  $q_n - j = k_n$  it can be calculated by:

$$I_n = I_{k_n} = \frac{\Gamma(k_n + \alpha_n + 1) \Gamma(k_n + \beta_n + 1)}{\Gamma(2k_n + \alpha_n + \beta_n + 2)} 2^{(k_n + \alpha_n + \beta_n + 1)} \quad (34)$$

while for the rest of the cases:

$$I_n = I_{k_n} \binom{q_n - j}{k_n} F_{21}(k_n - q_n + j, \alpha_n + k_n + 1, \alpha_n + \beta_n + 2k_n + 2, 2) \quad (35)$$

where  $F_{21}(\cdot, \cdot, \cdot, \cdot)$  is a Gaussian hypergeometric function [27].

One can see that  $S_{k_n, q_n}^G(\xi_n)$  in Eq. (20) and  $S_{k_n, q_n}^B(\xi_n)$  in Eq. (21) can be calculated without any integration but using explicit formulas (31) and (33), respectively. As a consequence, UECs  $U_{\mathbf{k}, s}$  in Eq. (19) can also be calculated this way for each function  $HC_r^{\text{ATFs}}(\omega_s, \boldsymbol{\xi}_r^{\text{ATFs}})$  and  $HC_r^{\text{CTF}}(\omega_s, \boldsymbol{\xi}_r^{\text{CTF}})$  what is performed in step 6 of our UEC approach shown in Fig. 2. In the final novel part of our UEC approach, shown in Fig. 2, we calculate PCE coefficients of  $HT(\omega_s, \boldsymbol{\xi})$  and perform elementary operations with orthogonal polynomials what is presented in the next subsection.

### 3.4. The PCE of a Telecommunication System Transfer Function

We take advantage of the fact that the transfer function of the telecommunication system is a sum of transfer functions associated with rays which originate in the point of EM field source and reach an observation point. Each of these transfer functions is the product of antennas transfer function associated with ray no.  $r$  and a transfer function of ray no.  $r$ , which are called by us,  $HC_r^{\text{ATFs}}(\omega_s, \boldsymbol{\xi}_r^{\text{ATFs}})$  and  $HC_r^{\text{CTF}}(\omega_s, \boldsymbol{\xi}_r^{\text{CTF}})$ , respectively. The transfer function associated with the ray no.  $r$  for pulsation sample  $\omega_s$  is defined as follows.

$$HC_r(\omega_s, \boldsymbol{\xi}_r) = HC_r^{\text{ATFs}}(\omega_s, \boldsymbol{\xi}_r^{\text{ATFs}}) \cdot HC_r^{\text{CTF}}(\omega_s, \boldsymbol{\xi}_r^{\text{CTF}}) \quad (36)$$

The method that we use to derive PCE coefficients of Eq. (36) is analogous to methods used in literature for calculation of PCE coefficients for dynamic systems, e.g., [23]. Let us assume that  $\boldsymbol{\xi}_r^{\text{ATFs}} = \{\xi_0, \xi_1\}$ ,  $\boldsymbol{\xi}_r^{\text{CTF}} = \{\xi_2, \xi_3\}$ , and  $\boldsymbol{\xi}_r = \{\xi_0, \xi_1, \xi_2, \xi_3\}$ , while the expansions of the functions  $HC_r^{\text{ATFs}}(\omega_s, \boldsymbol{\xi}_r^{\text{ATFs}})$ ,  $HC_r^{\text{CTF}}(\omega_s, \boldsymbol{\xi}_r^{\text{CTF}})$  are as follows:

$$HC_r^{\text{ATFs}}(\omega_s, \xi_0, \xi_1) \approx \sum_{\mathbf{j}} AH_{r, \mathbf{j}}^{\text{ATFs}} \cdot \Psi_{r, \mathbf{j}}^{\text{ATFs}}(\xi_0, \xi_1) \quad (37)$$

$$HC_r^{\text{CTF}}(\omega_s, \xi_2, \xi_3) \approx \sum_{\mathbf{k}} AH_{r, \mathbf{k}}^{\text{CTF}} \cdot \Psi_{r, \mathbf{k}}^{\text{CTF}}(\xi_2, \xi_3) \quad (38)$$

The goal is to expand function  $HC_r(\omega_s, \xi_0, \xi_1, \xi_2, \xi_3)$  into the following form:

$$HC_r(\omega_s, \xi_0, \xi_1, \xi_2, \xi_3) \approx \sum_{\mathbf{m}} AH_{r, \mathbf{m}} \cdot \Psi_{r, \mathbf{m}}(\xi_0, \xi_1, \xi_2, \xi_3) \quad (39)$$

where:  $\mathbf{j}$ ,  $\mathbf{k}$ ,  $\mathbf{m}$  are multi-indexes,  $\Psi_{r, \mathbf{m}}(\xi_0, \xi_1, \xi_2, \xi_3) = \varphi_{r, m_0}(\xi_0) \cdot \varphi_{r, m_1}(\xi_1) \cdot \varphi_{r, m_2}(\xi_2) \cdot \varphi_{r, m_3}(\xi_3)$ ,  $\Psi_{r, \mathbf{j}}(\xi_0, \xi_1) = \varphi_{r, j_0}(\xi_0) \cdot \varphi_{r, j_1}(\xi_1)$ ,  $\Psi_{r, \mathbf{k}}(\xi_2, \xi_3) = \varphi_{r, k_0}(\xi_2) \cdot \varphi_{r, k_1}(\xi_3)$ . When we substitute expansion in Eqs. (39), (37), (38) into Eq. (36), we obtain:

$$\sum_{\mathbf{m}} AH_{r, \mathbf{m}} \cdot \Psi_{r, \mathbf{m}}(\xi_0, \xi_1, \xi_2, \xi_3) = \sum_{\mathbf{j}} AH_{r, \mathbf{j}}^{\text{ATFs}} \cdot \Psi_{r, \mathbf{j}}^{\text{ATFs}}(\xi_0, \xi_1) \cdot \sum_{\mathbf{k}} AH_{r, \mathbf{k}}^{\text{CTF}} \cdot \Psi_{r, \mathbf{k}}^{\text{CTF}}(\xi_2, \xi_3) \quad (40)$$

In order to derive PCE coefficient of  $HC_r(\omega_s, \xi_0, \xi_1, \xi_2, \xi_3)$  with multi-index  $\mathbf{m}$ , we apply Galerkin projection to both sides of Eq. (40) using polynomial  $\Psi_{r, \mathbf{m}}(\xi_0, \xi_1, \xi_2, \xi_3)$  and associated joint PDF. When we take advantage of orthogonal property [12] of the polynomials, we obtain:

$$AH_{r, \mathbf{m}} = \sum_{\mathbf{j}} Hq_{\mathbf{m}, \mathbf{j}} \cdot AH_{r, \mathbf{j}}^{\text{ATFs}} \quad (41)$$

where:

$$Hq_{\mathbf{m}, \mathbf{j}} = \sum_{\mathbf{k}} AH_{r, \mathbf{k}}^{\text{CTF}} \alpha_{\mathbf{m}}(\mathbf{j}, \mathbf{k}, \mathbf{m}) \quad (42)$$

$$\alpha_{\mathbf{m}}(\mathbf{j}, \mathbf{k}, \mathbf{m}) = \frac{1}{\gamma_{r, \mathbf{m}}} \langle \Psi_{r, \mathbf{j}}^{\text{ATFs}}(\xi_0, \xi_1), \Psi_{r, \mathbf{k}}^{\text{CTF}}(\xi_2, \xi_3), \Psi_{r, \mathbf{m}}(\xi_0, \xi_1, \xi_2, \xi_3) \rangle \quad (43)$$

In the case when functions  $\Psi_{r,\mathbf{j}}^{\text{ATFs}}(\xi_0, \xi_1)$ ,  $\Psi_{r,\mathbf{k}}^{\text{CTF}}(\xi_2, \xi_3)$ ,  $\Psi_{r,\mathbf{m}}(\xi_0, \xi_1, \xi_2, \xi_3)$  belong to the same orthogonal bases, expression (43) can be easily calculated by the formula:

$$\alpha_{\mathbf{m}}(\mathbf{j}, \mathbf{k}, \mathbf{m}) = \begin{cases} 1, & \text{if } \{m_0, m_1\} = \{j_0, j_1\} \wedge \{m_2, m_3\} = \{k_0, k_1\} \\ 0, & \text{otherwise.} \end{cases} \quad (44)$$

When the lengths of multi-indexes  $\mathbf{j}$ ,  $\mathbf{k}$  and  $\mathbf{m}$  equal  $d^{\text{ATFs}}$ ,  $d^{\text{CTF}}$  and  $d = d^{\text{ATFs}} + d^{\text{CTF}}$ , respectively, the above formula can be generalized as follows:

$$\alpha_{\mathbf{m}}(\mathbf{j}, \mathbf{k}, \mathbf{m}) = \begin{cases} 1, & \text{if } \forall_{(0 \leq n \leq d^{\text{ATFs}}-1)} (j_n = m_n) \wedge \forall_{(0 \leq n \leq d^{\text{CTF}}-1)} (k_n = m_{n+d^{\text{ATFs}}}) \\ 0, & \text{otherwise.} \end{cases} \quad (45)$$

When polynomial chaos expansions of  $HC_r^{\text{ATFs}}(\omega_s, \boldsymbol{\xi}_r^{\text{ATFs}})$  and  $HC_r^{\text{CTF}}(\omega_s, \boldsymbol{\xi}_r^{\text{CTF}})$  include  $P^{\text{ATFs}}$  and  $P^{\text{CTF}}$  components, respectively, polynomial chaos expansion of  $HC_r(\omega_s, \boldsymbol{\xi}_r)$  includes  $P^{\text{ATFs}} \cdot P^{\text{CTF}}$  components. The vector of multi-index  $\mathbf{m}$  of each product in the left side of Eq. (40) is created by concatenation of vectors of multi-indexes  $\mathbf{j}$  and  $\mathbf{k}$  belonging to factors which are included in this product.

When polynomial chaos expansion of Eq. (36) for each ray in a wireless telecommunication system is known, we derive polynomial chaos expansion of Eq. (5). It is assumed by us that all random variables associated with antennas are independent. Let us assume that two rays lead from the point of source of EM field to the observation point. Then we have vectors of random variables  $\boldsymbol{\xi}_1^{\text{ATFs}}$ ,  $\boldsymbol{\xi}_2^{\text{ATFs}}$ ,  $\boldsymbol{\xi}_1^{\text{CTF}}$ ,  $\boldsymbol{\xi}_2^{\text{CTF}}$  on the right side of Eq. (5). Let us assume also in the first illustrative example that  $\boldsymbol{\xi}_1^{\text{ATFs}} = \{\xi_0\}$ ,  $\boldsymbol{\xi}_2^{\text{ATFs}} = \{\xi_1, \xi_2\}$ ,  $\boldsymbol{\xi}_1^{\text{CTF}} = \{\xi_3\}$ ,  $\boldsymbol{\xi}_2^{\text{CTF}} = \{\xi_3, \xi_4\}$ . Consequently, transfer function  $HT(\omega, \boldsymbol{\xi})$  depends on the vector of random variables  $\boldsymbol{\xi} = \{\xi_0, \xi_1, \xi_2, \xi_3, \xi_4\}$ , while its PCE for pulsation sample  $\omega_s$  can be given as follows:

$$HT(\omega_s, \boldsymbol{\xi}) \approx \sum_{\mathbf{m}_1} AH_{1,\mathbf{p}_1} \cdot \Psi_{1,\mathbf{p}_1}(\xi_0, \xi_3) + \sum_{\mathbf{m}_2} AH_{2,\mathbf{p}_2} \cdot \Psi_{2,\mathbf{p}_2}(\xi_1, \xi_2, \xi_3, \xi_4) \quad (46)$$

where multi-indexes  $\mathbf{p}_1$  and  $\mathbf{p}_2$ , using the notation as in Eqs. (39), (44), (45), are  $\{m_{1_0}, 0, 0, m_{1_1}, 0\}$  and  $\{0, m_{2_0}, m_{2_1}, m_{2_2}, m_{2_3}\}$ , respectively. All of the components of expansion (46) belong to the same orthogonal basis and have unique multi-indexes. It should be noted that  $\varphi_0(\xi) = 1$  for each orthogonal basis in gPC theory. Consequently, polynomials  $\Psi_{1,\mathbf{p}_1}(\boldsymbol{\xi})$  depend only on variables  $\xi_0$  and  $\xi_3$ , while polynomials  $\Psi_{2,\mathbf{p}_2}(\boldsymbol{\xi})$  depend on variables  $\xi_1$ ,  $\xi_2$ ,  $\xi_3$  and  $\xi_4$ . In the second illustrative example, we assume that  $\boldsymbol{\xi}_1^{\text{ATFs}} = \{\xi_0, \xi_1\}$ ,  $\boldsymbol{\xi}_2^{\text{ATFs}} = \{\xi_2, \xi_3\}$ ,  $\boldsymbol{\xi}_1^{\text{CTF}} = \{\xi_4, \xi_5\}$ ,  $\boldsymbol{\xi}_2^{\text{CTF}} = \{\xi_4, \xi_5\}$ . Consequently, the vector of random variables of transfer function  $HT(\omega, \boldsymbol{\xi})$  is  $\boldsymbol{\xi} = \{\xi_0, \xi_1, \xi_2, \xi_3, \xi_4, \xi_5\}$ . Then by analogy to expansion (46), we could write:

$$HT(\omega_s, \boldsymbol{\xi}) \approx \sum_{\mathbf{m}_1} AH_{1,\mathbf{p}_1} \cdot \Psi_{1,\mathbf{p}_1}(\xi_0, \xi_1, \xi_4, \xi_5) + \sum_{\mathbf{m}_2} AH_{2,\mathbf{p}_2} \cdot \Psi_{2,\mathbf{p}_2}(\xi_2, \xi_3, \xi_4, \xi_5) \quad (47)$$

where multi-indexes  $\mathbf{p}_1 = \{m_{1_0}, m_{1_1}, 0, 0, m_{1_2}, m_{1_3}\}$ ,  $\mathbf{p}_2 = \{0, 0, m_{2_0}, m_{2_1}, m_{2_2}, m_{2_3}\}$ ; however, expansion (47) includes components which have the same multi-indexes. The not unique multi-indexes are formed by  $m_{1_0} = 0$ ,  $m_{1_1} = 0$ ,  $m_{2_0} = 0$ ,  $m_{2_1} = 0$ ,  $m_{1_2} = m_{2_2}$ ,  $m_{1_3} = m_{2_3}$ . Consequently, the components of expansion (47) which have the same multi-indexes have to be added all together in order to derive polynomial chaos expansion of  $HT(\omega, \boldsymbol{\xi})$ .

Having in mind the two presented illustrative examples the following conclusion can be made. When two or more ray transfer functions  $HC_r^{\text{CTF}}(\omega, \boldsymbol{\xi}_r^{\text{CTF}})$  depend on the same vector of random variables then components of PCEs of  $HC_r^{\text{ATFs}}(\omega_s, \boldsymbol{\xi}_r^{\text{ATFs}}) \cdot HC_r^{\text{CTF}}(\omega_s, \boldsymbol{\xi}_r^{\text{CTF}})$ , which have the same multi-indexes, need to be collected in order to derive PCE of  $HT(\omega_s, \boldsymbol{\xi})$ . Then the analogous rule to this, which is given below Eq. (47), should be applied. In other cases, all components of PCEs of  $HC_r^{\text{ATFs}}(\omega_s, \boldsymbol{\xi}_r^{\text{ATFs}}) \cdot HC_r^{\text{CTF}}(\omega_s, \boldsymbol{\xi}_r^{\text{CTF}})$  become the components of PCE of  $HT(\omega_s, \boldsymbol{\xi})$ .

#### 4. NUMERICAL EXAMPLES

In order to examine the UEC approach presented in Section 3, we simulate creeping wave diffraction for the two-dimensional scenario shown in Fig. 3. We use the Uniform Theory of Diffraction (UTD) with

slope diffraction defined in the frequency-domain [28, 29] and a corresponding creeping ray trajectory in the scenario. Only the rays which give the major contribution to the overall field at the observation point of receiving antenna  $P_R$  are taken into account. The antenna position is established at point  $P_T$ .

The aim of the simulation is to analyze the worst-case scenario of EM wave propagation in the presence of exemplary convex objects. This would concern a scenario when the transmitting antenna and the receiving antenna are shadowed by convex objects. The diffraction takes place on a cascade of three cylinders, see Fig. 3. The objects are assumed to be perfect conductors. The radius of each convex object is 0.75 m. We assume that the centers of the objects lie in one line. The distance between the centers of each consecutive pair of objects equals 2 m.

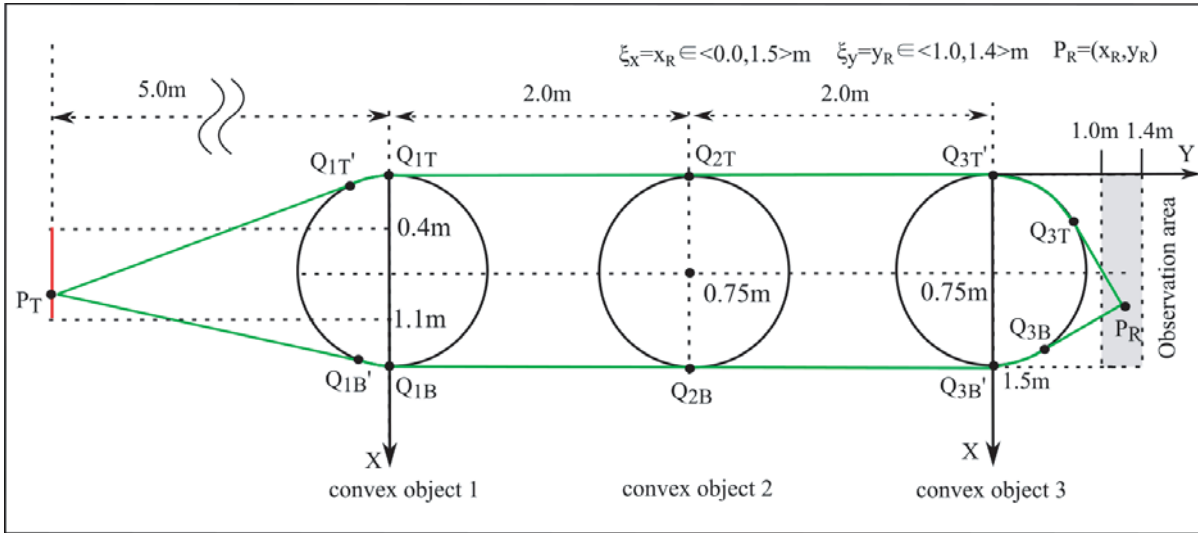


**Figure 3.** The scenario of a creeping wave propagating along three convex obstacles modeled by circular cylinders. The position of a transmitting antenna is represented by random variables  $\xi_x$ - $x$  dimension,  $\xi_y$ - $y$  dimension.

Transmitting antenna radiates EM wave whose frequency is 6 GHz. The point of a transmitting antenna  $P_T$  may change its position within the red line with a step of 2 cm (36 positions). The line is 5 m away from the center of convex object No. 1.

The coordinates of the position of a receiving antenna  $P_R$  are assumed to be random and may change their position within the observation area, which is a rectangle of the size 1.5 m  $\times$  0.4 m. The  $x$  and  $y$  coordinates of the receiving antenna position are represented by random variables  $\xi_x$  and  $\xi_y$ , respectively (see Fig. 3). We consider 300 nominal positions of a receiving antenna. Each nominal position lies at the center of a square of the size 0.02 m  $\times$  0.02 m. These sizes correspond to the uncertainties of a receiving antenna position in  $x$  and  $y$  domain ( $\pm 0.01$  m). The support of random variable  $\xi_x$  must be included within the limits  $1.00 \text{ m} \leq \xi_x \leq 1.40 \text{ m}$ , while the support of  $\xi_y$  within the limits  $0.00 \text{ m} \leq \xi_y \leq 1.50 \text{ m}$ . We also include uncertainties in magnitude and phase of transfer functions of transmitting and receiving antennas. The uncertainties of magnitude and phase of the transmitting antenna transfer function associated with the top ray in Fig. 3 are modeled by random variables  $\xi_1^{T, Mag}$  and  $\xi_1^{T, Ph}$ , respectively. The corresponding uncertainties of transmitting antenna transfer function associated with the bottom ray in Fig. 3 are modeled by random variables  $\xi_2^{T, Mag}$  and  $\xi_2^{T, Ph}$ , respectively. The analogous uncertainties of receiving antenna transfer functions are modeled by random variables  $\xi_1^{R, Mag}$  and  $\xi_1^{R, Ph}$ ,  $\xi_2^{R, Mag}$  and  $\xi_2^{R, Ph}$ . The influence of these uncertainties on the results of the worst-case analysis of the scenario in Fig. 3 is investigated in the simulation examples. We assume that all random variables in the described scenario have uniform PDFs. Using the above notation the transfer function of the telecommunication system for the scenario shown in Fig. 3 for each

of 15 positions of transmitting antenna is defined as follows.

$$HT(\omega, \boldsymbol{\xi}) = \sum_{r=1}^2 HC_r^{\text{ATFs}} \left( \xi_r^T, \text{Mag}, \xi_r^T, \text{Ph}, \xi_r^R, \text{Mag}, \xi_r^R, \text{Ph} \right) \cdot HC_r^{\text{CTF}}(\omega, \xi_x, \xi_y) \quad (48)$$

where

$$HC_r^{\text{ATFs}} \left( \xi_r^T, \text{Mag}, \xi_r^T, \text{Ph}, \xi_r^R, \text{Mag}, \xi_r^R, \text{Ph} \right) = \xi_r^T, \text{Mag} \cdot e^{-j \cdot \xi_r^T, \text{Ph}} \cdot \xi_r^R, \text{Mag} \cdot e^{-j \cdot \xi_r^R, \text{Ph}} \quad (49)$$

and  $HC_r^{\text{CTF}}(\omega, \xi_x, \xi_y)$  is the transfer function of ray no.  $r$  which is calculated using the uniform theory of diffraction [28]. The slope of the diffracted field is calculated as in [29]. We assume that an EM wave is TE-polarized. As we mentioned earlier we assume a two-dimensional case of EM wave propagation.

We analyze the worst-case scenario of an electric field amplitude for each  $0.02 \text{ m} \times 0.02 \text{ m}$  square at the receiving antenna site. We organize our calculations as follows. We assume that from the environmental protection perspective, for an electric field amplitude, the incident electric field cannot be larger than  $0 \text{ dBV/m}$  ( $1 \text{ V/m}$ ). We calculate the local minimum of an electric field amplitude for all nominal positions of the receiving antenna (300 positions). We calculate the local minimum value as the  $n$ th percentile of the calculated stochastic electric field amplitude. We repeat this procedure for all positions of the transmitting antenna. Then out of all local minima at each nominal position of the receiving antenna, we choose the minimal value, which is called the global minimum. If the global minimum for a given position of the receiving antenna is not lower than some threshold value associated with, e.g., receiver sensitivity, then the transmission between transmitting and receiving antennas will be successful for  $(100-n)\%$  of cases. Otherwise, this connection can be broken. We consider 5-th percentile of an electric field amplitude to calculate global minima. We will assume in the next subsections that the exemplary threshold value of electric field amplitude at the receiving site is  $-85 \text{ dBV/m}$ . The area for which the value of the global minimum of an electric field amplitude is below the threshold value is called the “Blind area”.

We present 7 simulation examples in the paper for 7 different ranges of uncertainties of antennas transfer functions. We will present the changes of the “Blind area” between the chosen simulation examples and the corresponding distribution of values of global minima for the observation area shown in Fig. 3. We show also the results of the relative error between UEC results and the Monte Carlo results for the chosen simulation examples. We do not show the error between UEC results and the gPC results; however, we note that this error is very small and that its maximum value is not bigger than  $0.5\%$  for all simulation examples. However, we do present the comparison of the times necessary to run the simulations using the Monte Carlo method, gPC approach and our UEC approach for all simulation examples in a tabular form.

As we mentioned in Section 3.2, we take advantage of the freeware Matlab-based package called UQLab [24] to obtain the results of the primary approximation for the UEC approach, as well as for numerical calculations of PCE coefficients in the gPC approach. We choose the orthogonal matching pursuit (OMP) method with Sobol indices calculation to calculate PCE coefficients in UQLab.

The values of parameters of PDFs assumed for the mentioned simulation examples are shown in Table 1. The lower and higher limits of supports of uniform random variables which model uncertainties of antennas transfer functions are denoted in Table 1 by  $c$  and  $d$ , respectively. The first column in Table 1 refers to the number of simulation example. The next 4 columns in Table 1 contain the pairs of  $c$  and  $d$  values. The first pair corresponds to the magnitude of antennas transfer functions, while the second to the phase of antennas transfer functions.

The values of parameters used for calculations of all of the simulation examples and times of simulations are given in Table 2. In the second and third column of Table 2, we present the times of Monte Carlo simulations and the number of MC samples used, respectively. In the next two columns, we give the corresponding data for the gPC approach. Abbreviation “Samp” means the number of samples which is used in the OMP method [24], while “Deg” means the maximum degree of an univariate polynomial in PCE expansion. The analogous information associated with the UEC approach is presented in the next two columns of Table 2. We performed calculations as in Eq. (47) for the UEC approach. For the case of the UEC approach, “Samp” means the sum of samples which are used in primary approximation for antennas transfer functions and rays transfer functions, while “Deg” has the same meaning as for the case of the gPC approach. The speedup provided by our UEC

**Table 1.** The values of parameters of PDFs assumed for the simulation examples.

Sim. Ex. No.	ATFs Magn. Uncertainty		ATFs Phase Uncertainty	
	$c$	$\frac{V/m}{V/m}$	$d$	$\frac{V/m}{V/m}$
1	1	1	0	0
2	0.90	1.10	-10	10
3	0.85	1.15	-20	20
4	0.80	1.20	-30	30
5	0.75	1.25	-40	40
6	0.70	1.30	-50	50
7	0.65	1.35	-60	60

**Table 2.** Parameters and times associated with calculations of the simulation examples.

Sim. Ex. No.	MC [s]	MC Samp	gPC [s]	gPC Samp (Deg)	UEC [s]	UEC Samp (Deg)	Speedup gPC/UEC	Speedup MC/UEC
1	8779	5000	1279	200(21)	157.58	600(17)	8.12	55.71
2	10825	6400	1799	400(21)	173.72	660(17)	10.36	62.31
3	13184	7700	2451	500(21)	182.76	690(17)	13.41	72.14
4	15478	9000	3264	580(21)	192.61	750(17)	16.95	80.36
5	18125	10500	4415	640(21)	203.48	750(17)	21.70	89.08
6	20518	11800	5915	710(21)	214.87	780(17)	27.53	95.49
7	22959	13100	8107	800(21)	227.18	780(17)	35.69	101.06

approach is presented in the last two columns of Table 2. The size of spatial support for the primary approximation of each ray transfer function is  $0.1\text{ m} \times 0.1\text{ m}$ .

As it is shown by the results included in Table 2, our UEC approach provides a substantial saving of simulation time for the case of worst-case analysis in a stochastic telecommunication system when compared to the gPC approach and especially to the Monte Carlo method. In our exemplary scenario, which is shown in Fig. 3, we considered 36 positions of a transmitting antenna and 300 nominal positions of a receiving antenna. As a consequence, we performed 10800 simulations of propagation of stochastic EM wave for the scenario shown in Fig. 3. The time reduction provided by our UEC approach is the larger the bigger is the number of simulations which are required to perform the worst-case analysis of a considered telecommunication system.

It is important to note that we use the gPC approach according to the diagram shown in Fig. 1. This approach implements the non-intrusive method for calculations of PCE coefficients. We could modify this approach by adding the steps analogous to the steps with numbers 3, 4, 6 and 7 of the UEC approach. Then the speedup of our UEC approach compared to this modified gPC approach is 4.63 for the case of deterministic antennas transfer functions (simulation example No. 1) and is similar for the case of the other 6 simulation examples. This speedup is obtained when the size of spatial support for the modified gPC approach is  $0.02\text{ m} \times 0.02\text{ m}$ . This speedup is about 50% lower when the size of spatial support for primary approximation of each ray transfer function is  $0.05\text{ m} \times 0.05\text{ m}$ . The times of calculations associated with the primary approximations of rays transfer functions are by far the biggest part of the whole simulation time. It is caused by high dynamics of each ray transfer function variation in the spatial domain.

The results corresponding to simulation examples No. 1 and No. 7 are presented in Figs. 4–7. The distribution of global minima obtained using the UEC approach presented in decibel scale with the

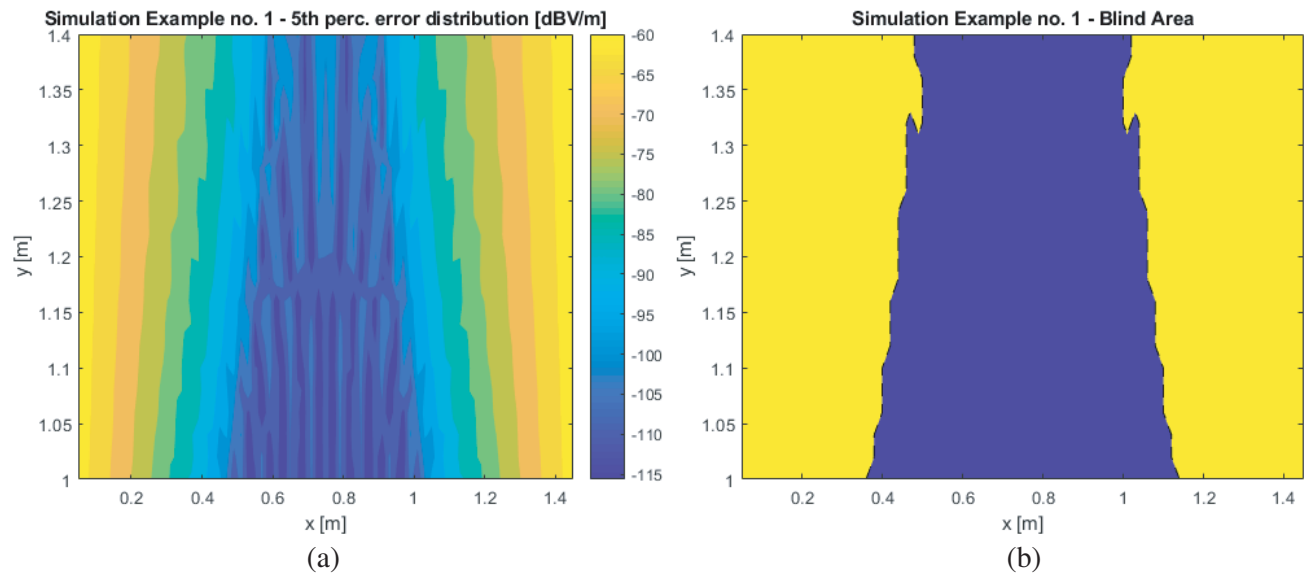


**Figure 4.** (a) The distribution of global minima obtained by using the UEC approach presented in the decibel scale and (b) the “Blind area” for simulation example No. 1.

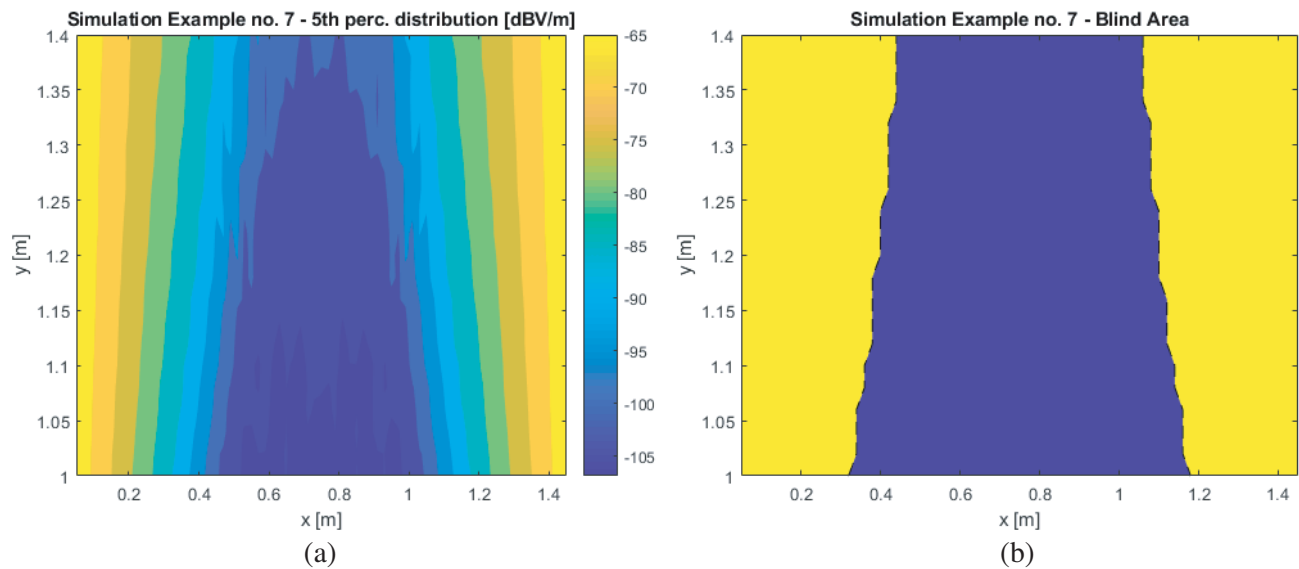


**Figure 5.** (a) The distribution of global minima obtained by using the UEC approach presented in the decibel scale and (b) the “Blind area” for simulation example No. 7.

corresponding “Blind area” for simulation examples No. 1 and No. 7 are shown in Fig. 4 and Fig. 5, respectively.

The figures show that the distribution of global minima is significantly changed when we consider the uncertainties of antennas transfer functions in the simulations. The “Blind area” increases when uncertainty of antennas transfer functions grows for the considered scenario. The relative error between UEC results and the Monte Carlo results of global minima for the case of simulation examples No. 1 and No. 7 are shown in Fig. 6(a) and Fig. 6(b), respectively, with MC results taken as a reference. The relative errors are calculated in % and derived for an electric field amplitude calculated using a natural scale. Exemplary histograms associated with these simulation examples are shown in Fig. 7. They are

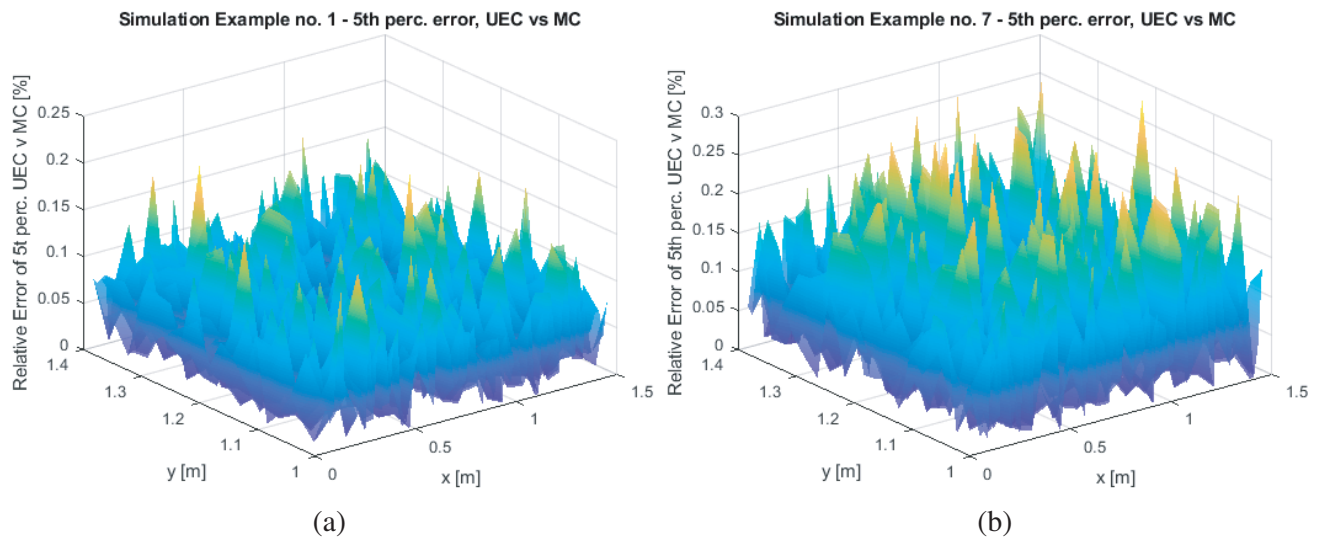


**Figure 6.** The relative error of UEC global minima results (a) for simulation example No. 1 and (b) for simulation example No. 7.

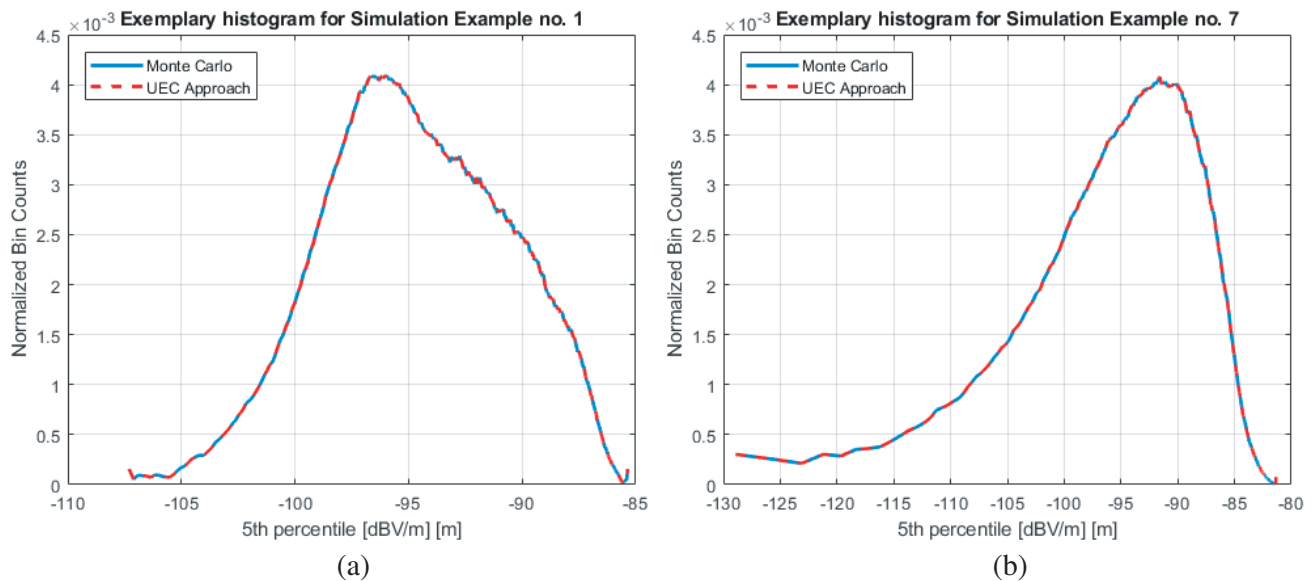


**Figure 7.** The smoothed histograms of an electric field amplitude at nominal observation point  $x = 1.26$  m,  $y = 0.75$  m calculated by using the MC method and the UEC approach for simulation examples (a) No. 1 and (b) No. 7.

calculated by using the MC method and the UEC approach for one nominal position of a receiving antenna,  $x = 1.26$  m and  $y = 0.75$  m. We used the same samples to the MC method and the UEC approach for the calculation of the histograms. The great agreement between the MC results and the UEC results is the consequence of very high accuracy of the primary approximation derived in step 5 of our UEC approach. We let the relative error of the primary approximation to be not bigger than 0.1%.

The analysis of the simulation examples showed that our UEC approach allows for a very significant reduction of time of random electromagnetic fields calculation for a telecommunication channel with randomly defined observation points. Such a significant reduction in the simulation time, enabled by our approach, results from the reduction of the number of necessary integrations or other numerical

operations [24]. It is achieved without deterioration of the accuracy of obtained PCE meta-models, and thus the accuracy of the distributions of a random amplitude of an electric field compared with the gPC and Monte Carlo approaches. We observed similar results of speedup and accuracy of analysis of random electric field for other simulation examples in which geometrical optics (GO) and UTD were used. However, they are not included in the paper because of the space limitation.

## 5. CONCLUSIONS

We presented in the paper a new PCE-based UEC approach to the fast and accurate simulation of worst-case scenario in a wireless telecommunication system. In this case, multiple simulations should be performed, each with a different set of PDFs of random variables. Namely, we presented in Section 3.3 new, closed-form analytical formulas which enable fast calculation of coefficients of polynomial chaos expansion. It is done in step 6 of our UEC approach. These formulas rely on primary approximations introduced in Section 3.2. The numerical calculation of primary approximation coefficients in Eq. (6) has to be performed once for each support introduced in Step 4 of the UEC approach. This process is by far the most time-consuming step in the UEC approach. In step 7 of the UEC approach, we proposed the novel intrusive method for calculation of PCE expansion of a stochastic EM field in a wireless telecommunication system. Our UEC approach requires the description of the transmission in the telecommunications system, i.e., its transfer function in the frequency domain which depends on random parameters (described using independent random variables). The approach relies on the nature of ray tracing simulation and on separating antennas transfer function and the ray transfer function for each ray. The analytical UECs, presented in Section 3.3, are dedicated to Gaussian and Beta distributions. These two probability densities cover a very wide range of probability densities considered in the literature for simulations of stochastic EM field distributions. It should be noted that uniform probability density can be modeled by Beta distribution as in the simulation examples presented in Section 4. The limitation of the UEC approach is related to the frequency of the EM field which needs to be expanded by using PCE. We observed that at about 30 GHz and higher frequencies the OMP, as well as the other non-intrusive methods of PCE coefficients calculation are hardly efficient. In order to obtain a sufficient quality primary approximation, very high order approximations need to be used. Consequently, simulation times dramatically increase. It is the common limitation of the gPC and UEC approaches. We are currently working on the application of our approach to the full-wave analysis (e.g., FDTD method, method of moment). It turns out that the application of the approach presented in this paper, using the so-called “primary approximations” and analytical formulas presented in this article, also gives a significant speedup of PCE meta-models calculation. The first results regarding the FDTD method are promising; however, they require further work and possible results will be published later.

## ACKNOWLEDGMENT

The work was supported by the Ministry of Science and Higher Education.

## REFERENCES

1. Alibakhshi-Kenari, M., M. Naser-Moghadasi, R. A. Sadeghzadeh, B. S. Virdee, and E. Limiti, “Traveling-wave antenna based on metamaterial transmission line structure for use in multiple wireless communication applications,” *AEUE Elsevier — International Journal of Electronics and Communications*, Vol. 70, No. 12, 1645–1650, 2016.
2. Alibakhshi-Kenari, M., M. Naser-Moghadasi, R. A. Sadeghzadeh, B. S. Virdee, and E. Limiti, “A new planar broadband antenna based on meandered line loops for portable wireless communication devices,” *Radio Science*, Vol. 51, No. 7, 1109–1117, 2016.
3. Alibakhshi-Kenari, M., M. Naser-Moghadasi, R. A. Sadeghzadeh, B. S. Virdee, and E. Limiti, “Periodic array of complementary artificial magnetic conductor metamaterials-based multiband antennas for broadband wireless transceivers,” *IET Microwaves, Antennas and Propagation*, Vol. 10, No. 15, 1682–1691, 2016.

4. Alibakhshi-Kenari, M., M. Naser-Moghadasi, R. A. Sadeghzadeh, B. S. Virdee, and E. Limiti, "New compact antenna based on simplified CRLH-TL for UWB wireless communication systems," *International Journal of RF and Microwave Computer-Aided Engineering*, Vol. 26, No. 3, 217–225, 2016.
5. Alibakhshi-Kenari, M., M. Naser-Moghadasi, R. A. Sadeghzadeh, B. S. Virdee, and E. Limiti, "Dual-band RFID tag antenna based on the hilbert-curve fractal for HF and UHF applications," *IET Circuits, Devices and Systems*, Vol. 10, No. 2, 140–146, 2016.
6. Schafer, T. M. and W. Wiesbeck, "Simulation of radiowave propagation in hospitals based on FDTD and ray-optical methods," *IEEE Trans. on Antennas and Propagation*, Vol. 53, No. 8, 2381–2388, 2005.
7. Hosseini Tabatabaei, S. A., M. Fleury, N. N. Qadri, and M. Ghanbari, "Improving propagation modeling in urban environments for vehicular ad hoc networks," *IEEE Trans. on Intelligent Transportation Systems*, Vol. 12, No. 3, 769–783, 2011.
8. Lertsirisopon, N., G. S. Ching, M. Ghoraiishi, J.-I. Takada, I. Ida, and Y. Oishi, "Investigation of non-specular scattering by comparing directional channel characteristics from microcell measurement and simulation," *IET Microwaves, Antennas and Propagation*, Vol. 2, No. 8, 913–921, 2008.
9. Ozgun, O. and M. Kuzuoglu, "Monte Carlo-based characteristic basis finite-element method (MCCBFEM) for numerical analysis of scattering from objects on/above rough sea surfaces," *IEEE Trans. on Geoscience and Remote Sensing*, Vol. 50, No. 3, 769–783, 2012.
10. Wagner, R. L., J. Song, and W. C. Chew, "Monte Carlo simulation of electromagnetic scattering from two-dimensional random rough surfaces," *IEEE Trans. on Antennas and Propagation*, Vol. 45, No. 2, 235–245, 1997.
11. Wiener, N., "The homogeneous chaos," *American Journal of Mathematics*, Vol. 60, No. 4, 897–936, 1938.
12. Xiu, D., *Numerical Methods for Stochastic Computation. A Spectral Method Approach*, Princeton University Press, New Jersey, 2010.
13. Edwards, R. S., A. C. Marvin, and S. J. Porter, "Uncertainty analyses in the finite-difference time-domain method," *IEEE Trans. Electromagn. Compat.*, Vol. 52, No. 1, 155–163, 2010.
14. Kersaudy, P., S. Mostarshedi, S. Sudret, and O. Picon, "Stochastic analysis of scattered field by building facades using polynomial chaos," *IEEE Trans. on Antennas and Propagation*, Vol. 62, No. 12, 6382–6393, 2014.
15. Boeykens, F., H. Rogieri, and L. Vallozzi, "An efficient technique based on polynomial chaos to model the uncertainty in the resonance frequency of textile antennas due to bending," *IEEE Trans. on Antennas and Propagation*, Vol. 62, No. 3, 1253–1260, 2014.
16. Larbi, M., I. S. Stievano, F. Canavero, and P. Besnier, "Identification of main factors of uncertainty in a microstrip line network," *Progress In Electromagnetics Research*, Vol. 162, 61–72, 2018.
17. Haarscher, A., P. De Doncker, and D. Lautru, "Uncertainty propagation and sensitivity analysis in ray-tracing simulations," *Progress In Electromagnetics Research M*, Vol. 21, 149–161, 2011.
18. Eldred, M. S., "Design under uncertainty employing stochastic expansion methods," *International Journal for Uncertainty Quantification*, Vol. 1, No. 2, 119–146, 2011.
19. Xiu, D., "Fast numerical methods for stochastic computations: A review," *Commun. Comput. Phys.*, Vol. 5, Nos. 2–4, 242–272, 2009.
20. Górnjak, P. and W. Bandurski, "A new approach to polynomial chaos expansion for stochastic analysis of EM wave propagation in an UWB channel," *Wireless Days*, Toulouse, March 23–25, 2016.
21. Górnjak, P. and W. Bandurski, "Universal approach to polynomial chaos expansion for stochastic analysis of EM field propagation on convex obstacles in an UWB channel," *12th European Conference on Antennas and Propagation, EuCAP 2016*, Davos, April 10–14, 2016.
22. Górnjak, P., "An application of universal polynomial chaos expansion to numerical stochastic simulations of an UWB EM wave propagation," *11th European Conference on Antennas and*

- Propagation, EuCAP 2017*, Paris, March 20–24, 2017.
23. Spina, D., D. Dhaene, and L. Knockaert, “Polynomial chaos-based macromodeling of general linear multiport systems for time-domain analysis,” *IEEE Trans. Microwave Theory and Techniques*, Vol. 65, No. 5, 1422–1433, 2017.
  24. Marelli, S. and B. Sudret, “UQLab user manual — Polynomial chaos expansions,” *Report UQLab-V1.0-104, Chair of Risk, Safety and Uncertainty Quantification*, ETH Zurich, 2017.
  25. Bella, T. and J. Reis, “The spectral connection matrix for any change of basis within the classical real orthogonal polynomials,” *Mathematics 2015*, Vol. 3, No. 2, 382–397, 2015.
  26. Weisstein, E. W., *CRC Concise Encyclopedia of Mathematics*, CRC Press, London, 2003.
  27. Forrey, R. C. and J. Reis, “Computing the hypergeometric function,” *Journal of Computational Physics*, Vol. 137, No. 1, 79–100, 1997.
  28. McNamara, D. A., *Introduction to the Uniform Geometrical Theory of Diffraction*, Artech House, Boston, 1990.
  29. Koutitas, G. and C. Tzaras, “A UTD solution for multiple rounded surfaces,” *IEEE Trans. on Antennas and Propagation*, Vol. 54, No. 4, 1277–1283, 2006.